Development and Production of Brake Pads from Palm Kernel Shell Composites

Z.U. Elakhame, O.A. Alhassan, A.E. Samuel

Federal Institute of Industrial Research, Oshodi, Lagos, Nigeria.

Email: ezeberu@yahoo.com, +2348038831703

Abstract— Development and production of asbestos-free brake pad using palm kernel shell (PKS) was studied with a view to replace the use of asbestos whose dust is carcinogenic. The PKS were sieve into sieve grades of 100,350,710µm and 1mm. The sieve PKS was used in production of brake pad in ratio of 20% resin, 10% graphite, 15% steel, 35-55% PKS and 0-20% SiC using compression moulding. The properties examined are microstructure analysis, hardness, compressive strength, density, flame resistance, water and oil absorption. The microstructure reveals uniform distribution of resin in PKS. The results obtained showed that the finer the sieve size the better the properties. The results obtained in this work were compared with that of commercial brake pad (asbestos based and optimum formulation laboratory brake pad Palm Kernel Shell based (PKS), the results are in close agreement. Hence PKS can be used in production of asbestos-free brake pad.

Keywords— Absorption (Oil & Water), Compressive strength, Density, Flame Resistance, Hardness, Microstructure, Palm kernel Shell, Porosity, Swell and Wear,

1 INTRODUCTION

Brake pads are one of the most important safety and performance components in automobiles.

The major component in the brake pad is the lining materials, which are categorized as metallic, semi-metallic, organic and carbon-based, depending on the composition of the constituent elements. Typical formulations consist of more than 10 ingredients, and more than 300 materials are in different brands **[1].** These ingredients are classified into four broad groups: binders, reinforcing fibres or structural materials, fillers, and frictional additives/modifiers, based on the major function they perform apart from controlling friction and wear performance. The binder holds the ingredients together, to maintain structural integrity of the brake lining under varying mechanical and thermal stresses. The structural materials provide the structural reinforcement to the composite matrix; fillers make up the free volume of the brake lining and friction modifiers stabilize the coefficient of friction and wear rates. These components perform synergistically in controlling friction and wear performance of the brake pad.

Asbestos had a few engineering properties that made it very suitable for inclusion in brake linings, and was the most preferred filler material up till 1989 **[2].** The use of asbestos is been avoided due to its carcinogenic nature **[1].** Therefore a new asbestos free friction material and brake pads has been developed.

Consequently, researchers have struggled to come up with an equally efficient alternative. Barites, mica, cashew dust, fly ash, ceramic fibre are some of the materials that have been considered for use as fillers **[2], [3].** In this research work, the use of milled palm kernel shell was contemplated on the basis of some of it engineering properties reported in the literature **[4]**

Although the use of asbestos for brake pads has not been banned, much of the brake pad industry is moving away from asbestos brake pads because of cancers.

Researches all over the world are focusing on ways of utilizing either industrial or agricultural wastes as a source of raw materials in the industry. These wastes utilization will not only be economical, but may also result to foreign exchange savings and environmental control.

Palm kernel shell is the residue fiber remaining when kernel is been crack from the shell.

Some palm kernel shell is burned in the open air or left to settle in waste ponds. This way, the Palm kernel processing industry's waste contributes significantly to green house effect **[5].**

1.1 Palm Kernel Shell as Brake Lining Ingredient

Palm Kernel Shell (PKS) is recovered as by-product in palm oil production. Large quantities of PKS are generated annually and only some fractions are used for fuel and other applications such as palliative for un-tarred road and in producing activated carbon.

The unused PKS are dumped around the processing mill, constituting environmental and economic liability for the mill.

Although, PKS must be ground into fine particles to be suitable for inclusion in brake lining, available information in the literature are on the ungrounded shell particles.

Coefficients of friction of PKS on metal surfaces were in the range of 0.37-0.52 **[4].** In contrast, friction coefficient in the range of 0.30-0.70 is normally desirable when using brake lining material [1]. It has been found **[1]** that incorporation of PKS in the production of structural light weight concretes increased the mechanical strength. Thus, PKS appeared suitable for use as base material in friction composites, because they are subjected to hard and variable braking forces.

[7] Reported that PKS did not change significantly in physical structure and weight, for appreciable time duration, when exposed to organic solvent. It is also important that the friction materials experience very little or no changes on contacting varying environmental conditions: wet or dry weather, or hydraulic fluid spilling over.

These observations therefore, stimulated the interest in considering PKS for use as friction material in brake lining. Hence, the aim of this research is to develop a new asbestos free brake pad from Palm kernel shell, which is readily available and non toxic.

EXPERIMENTAL

Materials

The materials used during the course of this work are: Phenolic resin (phenol formaldehyde), Palm kernel shell, steel dust, graphite and silicon carbide with compositional analysis are shown in Table 1 and Figure 1 below.

Figure.1. Photo of the ingredients

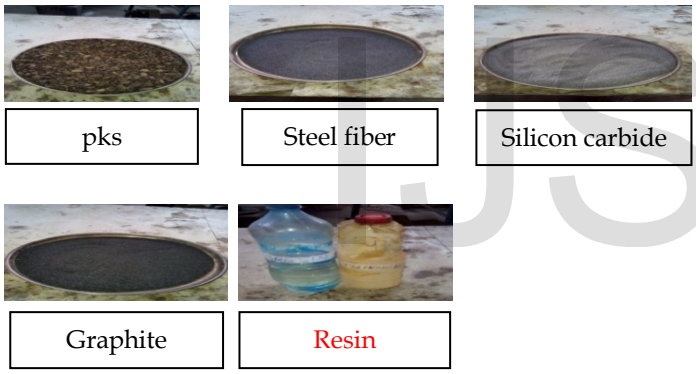

TABLE 1: ELEMENTAL COMPOSITION ANALYSIS OF PKS PARTICLES

S/No	Parameter	Level Detected (Palm Kernel Shell)	Unit
1	Ba(mg/kg)	ND	Wt%
2	Br(mg/kg)	0.005	Wt%
3	Ca(mg/kg)	0.028	Wt%
4	Cu(mg/kg)	0.009	Wt%
5	Cr(mg/kg)	0.002	Wt%
6	Fe(mg/kg)	0.006	Wt%
7	K(mg/kg)	0.005	Wt%
8	Mn(mg/kg)	0.002	Wt%
9	Ni(mg/kg)	ND	Wt%
10	Se(mg/kg)	0.003	Wt%
11	Sr(mg/kg)	ND	Wt%
12	V(mg/kg)	ND	Wt%
13	Zn(mg/kg)	0.074	Wt%

Raw Material Preparation

A 150 kg quantity of palm kernel shells was obtained from a local processing mill at Ota community in Ogun state. The sample was cleaned and sun-dried to remove kernel, nuts, extraneous materials and contaminating kernel oil. The shells was ground into powder using a hammer mill (Model 000T, Puissance: 1.5KV, No 13634), ball milling machine (Model 87002 Limoges-France, A50……43) and then sieved into different sieve sizes of aperture 1mm, 710µm, 355µm, and 100µm. Using a set of **BS 410 standard sieves (Endecotts Ltd., London**) **[8]** in the brake lining formulation.

Production of brake pad consists of a series of unit operations including mixing, cold and hot pressing, cooling, post-curing and finishing **[8].** The constituent ingredients, PKS, steel dust, graphite, silicon carbide, and resin. Different composition and sieve grades (i.e. 1mm, 710µm, 355µm, and 100µm) of PKS, steel dust, graphite, silicon carbide powder and resin were added together in the ratio shown in table.2. The combination were properly dry mixed in a mixer for 20 minutes (Model 89..2 Ridsdale & Co ltd, Middlesbrough.Eng.) until a homogenous component was formed and transferred into a mould for cold pressed with a Hydraulic press (Model Pi00eh-Type, 100T-Capacity, Serial No-38280) at 80KN/cm^2 and then conveyed into electric oven (Model Memmert, Western Germany) at a temperature of 150^{o}C after which it was hot pressed at 100KN/cm^2 pressure for 2 minutes. After removing from hot mould, the brake pad was cured in an oven at a temperature of 120^{o}C for 8 hours **[9], [10].** The produced samples are shown in Figure 2.

TABLE 2: FORMULATION

S/N	Ingredients	A	B	C	D	E
1.	PKS	35	40	45	50	55
2.	Resin	20	20	20	20	20
3.	Steel dust	15	15	15	15	15
4.	Graphite	10	10	10	10	10
5.	Silicon carbide (SiC).	20	15	10	5	0

FIGURE 2: PHOTO OF THE PRODUCED SAMPLES (PRODUCTS)

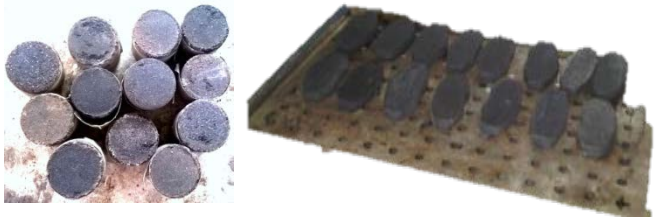

Sample Characterization

Brinell Hardness Test

The resistance of the composites to indentation was carried out through the Brinell hardness testing equipment to BS240, using a Tensometer (M500-25KN, Gunt Hamburg Hardness Tester and WP300) pressing hardened steel ball with diameter *D* into a test specimen. Based on ASTM specification, a 10 mm diameter steel ball was used, and the load applied P was kept stable at 3000 kg/f. The diameter of the indentation d was measured along two perpendicular directions, using an optical micrometer screw gauge. The mean value was taken and incorporated into Eqn. 1 to obtain the Brinell Hardness Number (BHN).

$$BHN = 2P \div \pi D\,(D - \sqrt{D^2 - d^2}) \quad \ldots\ldots (1)$$

Where P is the load applied, D is the diameter of hardened steel ball into a test specimen and d is the diameter of indentation

Tensile Strength Test

The tensile strength test value was carried out in the conversion table of Brinell hardness values. The formula is shown in Eqn 2 below.

$HV = 1.854P \div d12$ TS (Mpa) $3.45 \times HB$

TS (Psi) $500 \times HB$…… (2)

Where HB is the Brinell hardness values, *P is the load applied and d is the diameter of indentation*

Compressive Strength Test

The compressive strength test was done using the Tensometric Machine. The samples of diameter 29.40mm was subjected to compressive force, loaded continuously until failure occurred. The load at which failure occurred was then recorded.

Flame Resistance Test

Weigh about 1.20g ± 0.1g of the samples in a cooled crucible previously oven dried by heating in a furnace at 550^{0}C for 1 hour. Then the samples were charred by heating in a hot plate thereafter, the charred samples were taken into the furnace and heated at 550^{0}C for 1 hour. Then cooled in a dessicator and weigh. This cycle of heating, cooling and weighing were repeated until a constant weight was obtained.

Calculation:

$$\% \text{ ash} = \frac{W_2 - W_0}{(W_1 - W_0)} * 100 \quad \ldots\ldots (3)$$

Where W_0=weight of empty crucible

W_1=weight of crucible + sample

W_2=weight of crucible and residue i.e. after cooling.

Water and Oil Absorption (Thickness Swell Test)

The water and oil (10W-40) absorption of the samples were determined by soaking the samples into water and oil for 24 hours. Before the tests the weights of the samples were determined, after oven -drying of the samples at 100^{o}C for 24 hours the weights of samples were measured.

The percentage of absorption was determined **[10]**. The formula is shown in below in Eqn. 4.

$$\text{Thickness swell } (t) = M2 - M1 \div M1 \times 100 \quad \ldots\ldots (4)$$

Where M_2 is the mass of test piece after absorbing oil and water (g), M_1 is the mass of test piece (g)

Density Test

The true density of the samples was determined by weighing the samples mass on a digital weighing machine and divided by measuring their volume by liquid displacement method. The formula is show in Eqn. 5 below.

$$\text{Density } (\varrho) = M \div V \times 10 \quad \ldots\ldots (5)$$

Where M is the mass of test piece (g) and V is the measuring volume of test piece (cm^3) by liquid displacement method

Specific Gravity Test

Subsequently their specific gravities were determined by dividing the unit weight of the sample in air by the unit weight of the sample in air and water. The formula is show in Eqn 6 below.

$$\text{Specific gravity } (sg) = Wa \div (Wa - Wb) \quad \ldots\ldots (6)$$

Where Wa is the weight of sample in air (g); and Wb is the weight of sample in water (g).

Wear Rate Test

The wear rate for the samples were measured using pin on disc machine by sliding it over a cast iron surface at a load of 10N and 20N, sliding speed of 125rev/min and250rev/min, and sliding distance of 2000m and 4000m. All tests were conducted at room temperature. The initial weight of the samples was measured using a single pan electronic weighing machine with an accuracy of 0.01g. During the test, the pin was pressed against the counterpart rotating against a cast iron disc (hardness 65 HRC) of counter surface roughness of 0.3μm by applying the load. A friction detecting arm connected to a strain gauge held and loaded the pin samples vertically into the rotating hardened cast iron disc. After running through a fixed sliding distance, the samples were

removed, cleaned with acetone, dried, and weighed to determine the weight loss due to wear. The differences in weight measured before and after tests give the wear of the samples. The formula used to convert the weight loss into wear rate is **[11].**

Wear rate = Wear rate = S/W……. (7)

Where ΔW is the weight difference of the sample before and after the test in mg, S is total sliding distance in m.

Micro-structural Analysis

The microstructural analyses of the samples were carried out by grinding the samples using 300, 400, and 600 grit papers respectively. Dry polishing was then carried out on these samples and the internal structures were viewed under the computerized Metallurgical microscope **[1].**

Swell Growth Analysis

Dimensional stability of the friction composite when subjected to changes in temperature and humidity was quantified by measuring its percentage swell growth **[13]**. The thickness of the sample before being introduced into an oven T_{bo} was measured with a vernier caliper with accuracy of ±0.001 mm. The temperature in the oven was stabilized at 205°C and the sample, on a steel tray, was kept inside the oven for one hour. The thickness of the sample after being withdrawn from the oven and allowed to cool at room temperature for 20 minutes *Tc* was noted.

The percentage of swell (*SP)* was computed as:
$(Tc - T_{bo}) \times 100 \div Tbo$ …… (8)

Where Tbo is the thickness of the samples before being introduced into an oven while Tc is the thickness of the samples after being withdrawn from the oven and allowed to cool at room temperature for 20 minutes

Porosity

A sample of diameter 29.40mm with a different height thickness of as thick as possible was used. The specimens were weight to the nearest in mg, and then soak in oil and water container at 90-100oC for 8hrs. The samples were leave for 24hrs and then taken out from the oil container. Finally, the test samples were weight to the nearest mg. this formula was noted in Eqn 9.

Porosity $(\varrho) = M_2 - M_1 \div D \times 100 \div V$…….. (9)

D is the density of test oil and water M_2 is the mass of test piece after absorbing oil and water (g), M_1 is the mass of test piece (g) and V is the volume of test piece (cm^3).

TABLE 3: THE PRODUCTS ARE IN COMPLIANCE WITH NATIONAL AND INTERNATIONAL STANDARDS

S/N	Test procedure	Standards
1	Specific Gravity	MS 474:PART 1: 2003
2	Rockwell Hardness Test	MS 474:PART 2: 2003
3	Compressive Strain Test Method	MS ISO 6310:2003, PART 4
4	Internal Shear Strength of Lining Material	MS ISO 6311:2003, PART 5
5	Shear Test Procedure	MS ISO 6312:2003, PART 6
6	Resistance to Water, Saline Solution, Oil & Brake Fluid	MS ISO 6314:2003, PART 8
7	Assessment of Friction Materials and Wear/ Microstructure	MS 474:PART 10: 2003
8	Determination of Thermal Conductivity	ISO 7882 : 1986
9	Porosity Measurement	JIS D 4418 – 1996
10	Swell, Growth and Dimensional Stability	SAE J 160 Jun 80
11	Dynamometer Noise Matrix Test	SAE J2521
12	Dynamometer Brake Effectiveness Test	SAE J2522
13	Vehicle Braking Test	ECE R13
14	Replacement Brake Lining Assemblies	ECE R90
15	Field Test on LRT Test Track	Company's Specifications
16	Ash test	SAE J160 Jun80

RESULTS AND DISCUSSION

Figures and Tables

Figures *Figs* 4a), b), c), d) & e) -8a), b), c), d), e), za & zb have showed the microstructure of the samples. Microstructure of 100μm, 355μm, 710μm and 1mm sieve grade sample(X100). Showing uniform dark red region of resin and white region of Palm kernel shell. The microstructure of the Palm kernel shell and asbestos based brake lining before and after wear test are shown in *Figs Figs* 4a), b), c), d) & e). -8a), b), c), d) & e), za & zb.. It is clear that before wear test takes place; it is easy to identify the various ingredients in the friction element. From *Fig*. 4a), b), c), d), -8a), b), c), d) & Za (Asbestos-based) particle is surrounded by copper dust and other unidentifiable elements. *Fig*. 7.b, presents asbestos fibres surrounded by

many other ingredients too. Once wear takes place, the impact of friction on friction composites has a double character: alterative for phases on friction surfaces and damaging for friction surfaces; voids are generated after wear test on both surfaces of *Figs* 4a), b), c), d) & e) -8a), b), c), d), e), & zb. In the asbestos-based and PKS-based friction composite (*Fig*. 4a), b), c), d) & e) -8a), b), c), d), e), & zb), steel particles are plastically deformed and smeared. Grooves parallel to disk rotation appear in both base materials.

From the microstructure there is more uniform distribution of the resin with the PKS as the particles size of the PKS decreased. This is as a result of proper bonding between the PKS and the entire composition as the sieve grade decrease and also closer inter-packing distance. This can be appreciable if one compares Figure 4a).100µmA with Figure7a).1mmA on Surfaces of unworn friction composites (before wear) and Fig. 5a, 5b, 5c, 5d, & 5e: Surfaces of worn friction composites (after wear) with Fig. 8a, 8b, 8c, 8d & 8e.

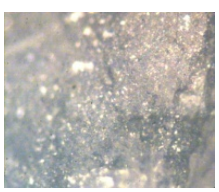

5a).355µmA

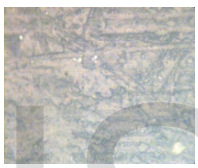

6a).710µmA

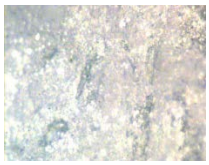

7a).1mmA

(Za). Asbestos-based
(Koya, O. A. , Fono, T. R).

FIGURE 4A, 5A, 6A, 7A & ZA: SURFACE OF UNWORN FRICTION COMPOSITES (BEFORE WEAR)

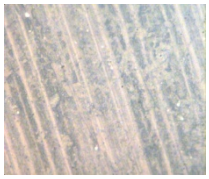

5a).100µmA

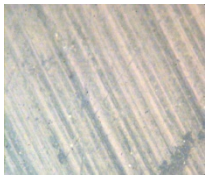

5b). 100µmB

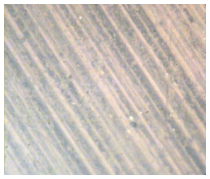

5c). 100µmC

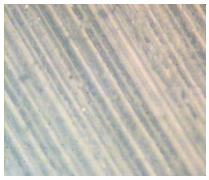

5d). 100µmD

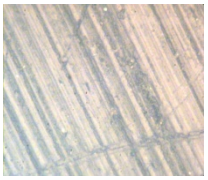

5e). 100µmE

FIGURE 5A, 5B, 5C, 5D & 5E: SURFACE OF WORN FRICTION COMPOSITES (AFTER WEAR)

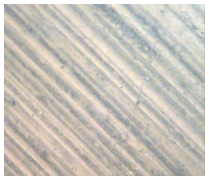

6a). 355µmA

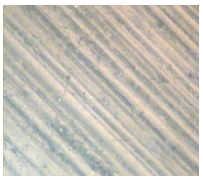

6b). 355µmB

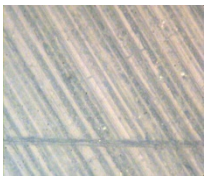

6c). 355µmC

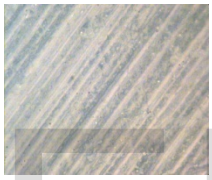

6d).355µmD

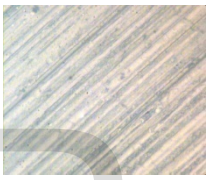

6e). 355µmE

FIGURE 6A, 6B, 6C, 6D & 6E: SURFACE OF WORN FRICTION COMPOSITES (AFTER WEAR)

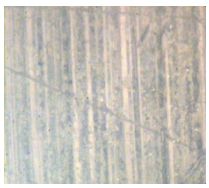

7a). 710µmA

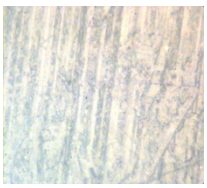

7b). 710µmB

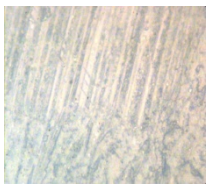

7c). 710µmC

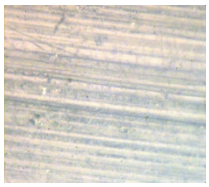

7d). 710µmD

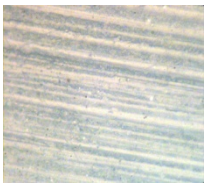

7e). 710µmE

FIGURE 7A, 7B, 7C, 7D & 7E: SURFACE OF WORN FRICTION COMPOSITES (AFTER WEAR)

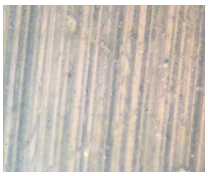

8a).1mmA

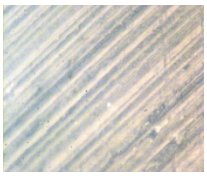

8b).1mmB

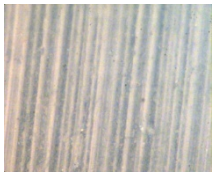

8c).1mmC

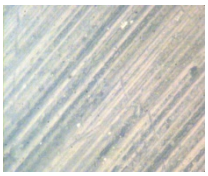

8d).1mmD

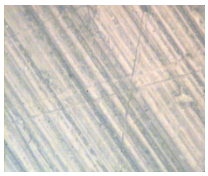

8e).1mmE

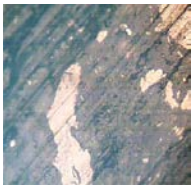

(Zb). Asbestos-based
(Koya, O. A. , Fono, T. R).

FIGURE 8A, 8B, 8C, 8D, 8E & ZB: SURFACE OF WORN FRICTION COMPOSITES (AFTER WEAR)

2.2 Brinell Hardness Test

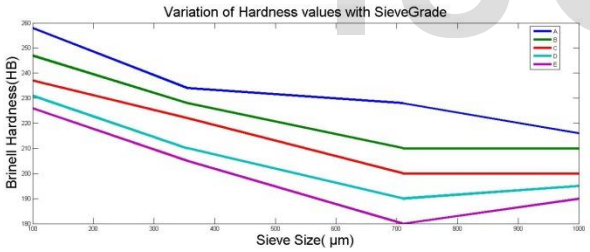

Figure 9

Figure 9 show the result of the Brinell hardness with sieve size particle. The sample with 100µm sieve grade of different proportion from A-E has the highest hardness value of 125HBN, 119HBN, 115HBN, 112HBN & 110HBN. A sharp drop in hardness was observed in the samples with higher sieve grades (355µm, 710µm & 1mm). The high hardness for the 100µm sieve grade was as a result of reduced particle size of Palm kernel shell i.e. increases in surface area which resulted to increase bonding ability with the resin. The hardness value for this material was compared with other materials from other researches [12], [13] as shown in the Table7 which indicated an acceptable result with the findings of other researchers. Figure.10 showed the compressive strengths of the produced samples. From the results similar trend with that of hardness values was observed that is compressive strength increases with decreased in sieve size of the samples.

2.3 Compressive Test

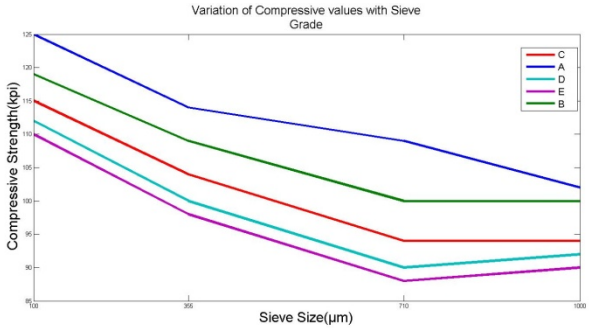

Figure 10

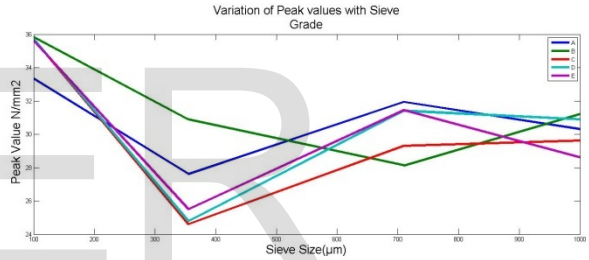

Figure 11

Figure 10 and 11 shows the result of the compressive strength and peak value with sieve size. The 100µm sieve grade also has the highest compressive strength of 125N/mm² and peak value of 35.825N/mm². The gradual decrease in compressive strength and peak value as the sieve size increases can be attributed to the decreasing surface area and pore packaging capability of the Palm kernel shell particles in the resin. Hence, compressive strength increases as particle size of palm kernel shell decreases.

2.4 Density Test

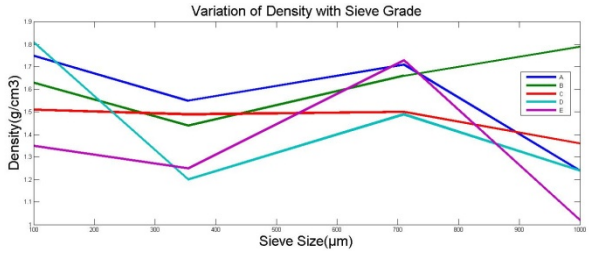

Figure 12 shows the result of the density with sieve size. The density deceased as the sieve size of the palm kernel shell

particles increases in the composition.
The decreased in density can be attributed to the increases in particle size i.e. increased packing of PKS. The 100μm has the highest density which is as a result of closer packing of palm kernel shell particles creating more homogeneity in the entire phase of the composite body [12].

2.5 Wear Rate

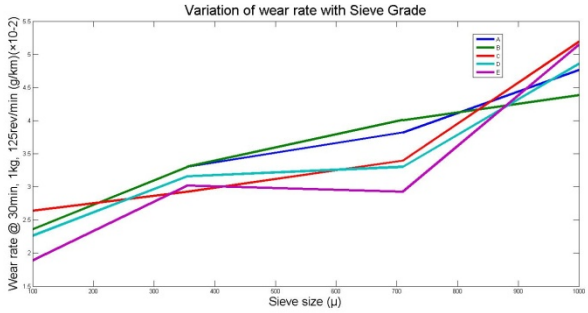

Figure 13

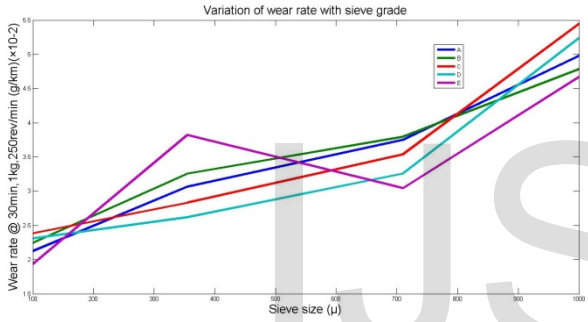

Figure 14

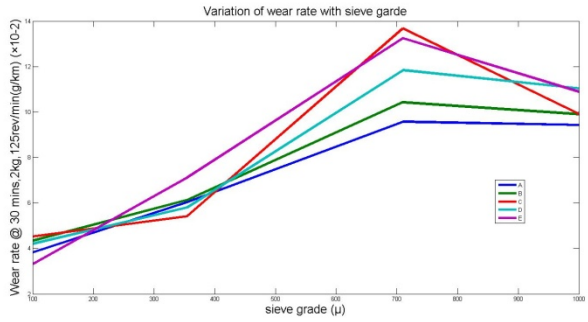

Figure 15

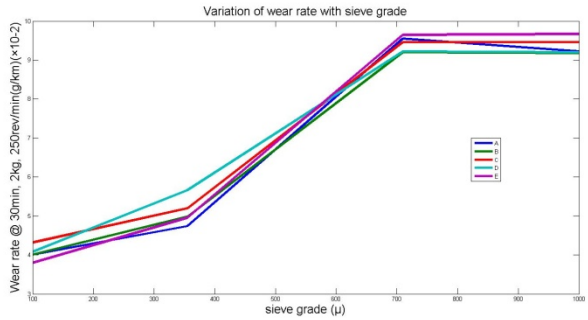

Figure 16

Figure 13-16 shows the wear rate result of the produced samples. The figure shows decrease in wear rate as the sieve grade of PKS increases. This resulted to higher/ closer packing which has affected stronger binding of PKS within the composition. This may also be due to high hardness values and compressive strength of the samples as sieve size is decreased.

2.6 Porosity

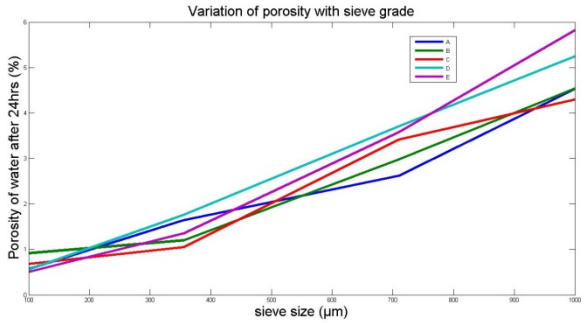

Figure 17

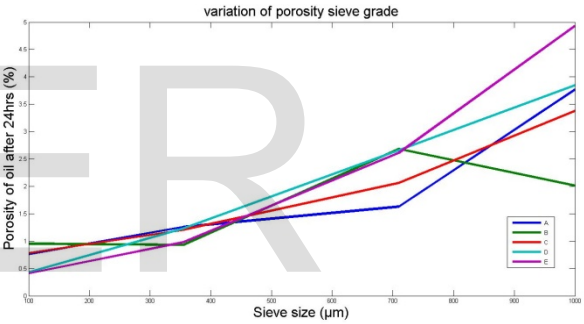

Figure 18

Figure 17 and 18 shows the result of the porosity with sieve size.
Those properties increased as the sieve grade increases which can eventually be attributed to the increases pores as sieve size increases. These results are in par with the earlier observation of Refs. [1-5]. It can be seen from the result that sample with 100 μm gave the best properties as a result of a very good dispersion of PKS particles as shown by the white region and dark region resin(see Figure 4a-8e) which led to a better interfacial bonding of the resin and the PKS particles as seen in subsequent samples.

Water and Oil Absorption (Thickness Swell) Test

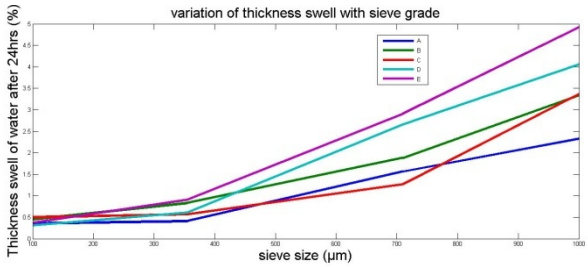

Figure 19

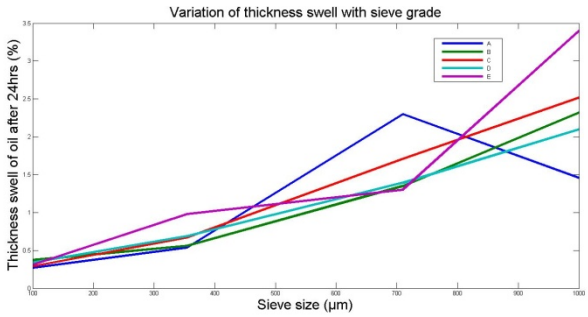

Figure 20

Figure 19 and 20 shows the graph for water absorption (thickness swell) for different composition of raw materials. From the graph, it can be seen that samples with 100 µm shows the higher value while from 355µm -1mm shows the lower value of water content. The increase in size of the PKS content will result in more water absorption because more pores are observed. This result was influenced by porosity and void formed in the brake pad samples. The water absorption decreased when increasing the PKS content. Theoretically, lower water absorb to the brake pad will result in higher friction coefficient and wear rate due to higher contact areas between the mating surface.

2.7 Specific Gravity Test

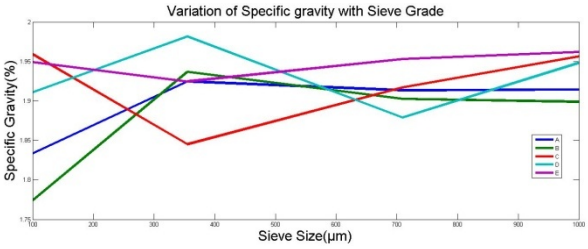

Figure 21

Figure 21 shows the result of the specific gravity with sieve size.

The decreased in specific gravity can be attributed to the increases in particle size i.e. increased packing of PKS. The particles size of 100µm-355µm has the highest density which is as a result of closer packing of PKS particles creating more homogeneity in the entire phase of the composite body [1].

2.8 Swell Test

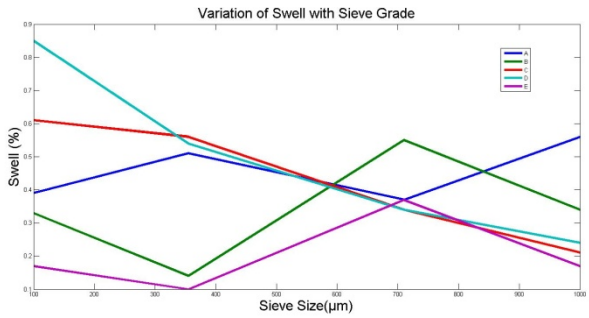

Figure 22

Figure 22 shows the result of the swell samples with sieve size. It can be seen from the graph that all samples have similar swell properties as a result of a very good dispersion of PKS particles which led to a better interfacial bonding of the resin and the other proportion particles as seen in subsequent samples. This has prove that particle size have no effect on swell (temperature).

2.9 Flame Resistance Test

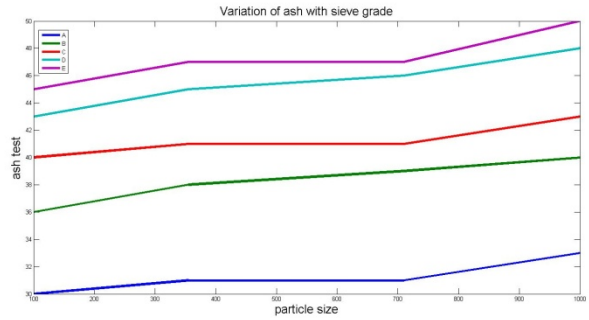

Figure 23

Figure 23 has shown the flame resistance of the produced samples, and it can be seen from the graph as the properties increased so as the sieve grade increases which can eventually be attributed to the increases pores as sieve size increases. It can also be observed from the result that samples with 100µm gave the best properties as a result of a very good dispersion of decreased in size particles.

TABLE 4: SUMMARY OF RESULT FINDINGS COMPARED WITH EXISTING ONES (1)

S/N	PROPERTY	BRAKE PAD COMMERCIAL (ASBESTOS BASED)	NEW FOMULATION LAB. BRAKE-PAD (PKS)
1	Hardness (at 3000kgH)	101	226-258
2	Compressive strength	110	110-125
3	Density	1.320	1.350-1.750
4	Assessment of foreign materials and wears / microstructure	(g/km*10^{-2}) 3.800	(g/km*10^{-2}) 1.887-2.359
5	Porosity Measurement Water: Oil	0.52 0.61	0.50-0.57 0.41-0.76
6	Resistance to water, saline Water: solution, oil, & brake fluid Oil	0.37 0.29	0.31-0.36 0.27-0.31
7	Specific gravity	1.7987	1.8333-1.9492
8	Swell measurement	0.28	0.17-0.39
9	Flame resistance test at 1 hour	Charmed with 54% ash	Charmed with 30-40 ash

The result of this research work indicates that samples containing 100µm of formulation (A-E) gave better properties than other samples like 355µm, 710µm and 1mm size particles from formulation (A-E) tested. Hence, the lower the sieve grades of PKS, the better the properties. The 100µm sieve size results were compared with that of commercial brake pad (asbestos based) and new formulation laboratory brake pad (Palm Kernel Shell) based as shown in the Table 14, which were tested under similar conditions.

The results are in close agreement. Hence asbestos free brake pad can be produced with 100µm sieve size formulation. Taking into consideration, all the desired dimensions of the brake pad, a protype of infinity (QX) and pathfinder jeep brake pad of length of 131mm, width of 50mm and depth of 8mm, the friction material was produced with this 100µm sieve size formulation (see Table 2). The produced protype were carried out with field test to show that the formulation can be used in the production of automotive brake-pad.

Produced PKS brake pads

4 CONCLUSION

From the observation and discussion of this research work the following conclusions can be made:

1. The samples, 100µm sieve grade of palm kernel shell gave the best properties in all.
2. Compressive strength, hardness, densities and porosity of the produced samples were seen to be decreasing with increase in sieve grade while there oil soak, water soak, wear rate and percentage charred increased as sieve grade increased.
3. Based on the above test properties of these brake pads composite using palm kernel shell as filler can be effectively used as an alternative to existing fillers, such as asbestos, in brake pad composites.

REFERENCES

[1.] V. S. Aigbodion., U. Akadike (development of asbestos - free brake pad using bagasse). *Tribology in industry*, Volume 32, No. 1, 2010.

[2.] Mohanty, S., Y.P. Chugh, 2007. Development of fly ash-based automotive brake lining. Tribol Int, 40: 1217-24.

[3.] Chan, D., G.W. Stachowiak, 2004. Review of automotive brake friction materials. J Automob Eng Proc Inst Mech Eng Part D, 218.

[4.] (Koya *et al*., 2004), Seperation theory for palm kernel and shell mixture on a spinning disc.

[5.] Mathur, R.B. Thiyagarajan, P. and Dhami, T.L. (2004). Controlling the hardness and Tribological Behaviour of Non-asbestos Brake Lining Materials for Automobiles. Journal of Carbon Science, vol. 5, No. 1, 6- 11.

[6] W. Österle A.I. Dmitriev, Functionality of conventional brake friction materials – Perceptions from findings observed at different length scales

[7.] (Akporhonor *et al*, 2007), international journal of material and mechanical engineering

[8.] (Gurunath and Bijwe, 2007), journal of engineering

tribology
[9] S.Y. Aku, D.S. Yawas; P.B. Madakson; and S.G. Amaren, Characterization of Periwinkle Shell as Asbestos Free Brake Pad Materials
[10] Sasaki, Y, Yanagi, M., Todani, Y. and Mita, T,(2000), Review of automotive brake friction materials
[11.] Osterle, W., Griepentrog, M., Gross, T. And Urban. I(2001), microstructural aspects controlling friction and wear of brake pads
[12.] Osterle, W., Griepentrog, M., Gross, T. and Urban. I(2001) Chemical and microstructural changes induced by friction and wear of brakes, Wear, 251, 1469–1476.
[13.] Blau, P. J (2001). Compositions, Functions and Testing of Friction Brake Materials and their Additives. Being a report by Oak Ridge National Laboratory for U.S Dept. of Energy.
[14.] [(Khan *et al*., 2006; Ayruliris, 2008, Palm kernel shell in the manufacture of automotive brake pad).
[15.] Ramousse, S., J.W. Hoj, O.T. Sorensen, 2001. Thermal Characterization of Brake Pads, Journal of Thermal Analysis and Calorimetry, 64: 933-943
[16.] Dagwa, I. M, and Ibhadode, A.O.A. (2006) Determination of Optimum Manufacturing Conditions for Asbestos-free Brake Pad using Taguchi Method, Nigerian Journal of Engineering Research and Development, Basade Publishing Press Ondo, Nigeria Vol. 5, No. 4, 1-8.
[17.] Satapathy, B.K., 2002. Performance analysis of non-asbestos fibre reinforced organic friction materials. Ph.D. thesis, IIT Delhi.
[18.] Dagwa, I.M. and Ibhadode, A.O.A. (2005). Design and Manufacture of Experimental Brake Pad Test Rig Nigerian Journal of Engineering Research and Development , Basade Publishing Press Ondo, Nigeria, Vol.4, No. 3. 15-24.